

# Analysis of Gamma-Ray Spectra Using Levenberg-Marquardt Method

A. H. Fatah, A. H. Ahmed

**Abstract**—Levenberg-Marquardt method (LM) was proposed to be applied as a non-linear least-square fitting in the analysis of a natural gamma-ray spectrum that was taken by the Hp (Ge) detector. The Gaussian function that composed of three components, main Gaussian, a step background function and tailing function in the low-energy side, has been suggested to describe each of the  $\gamma$ -ray lines mathematically in the spectrum. The whole spectrum has been analyzed by determining the energy and relative intensity for the strong  $\gamma$ -ray lines.

**Keywords**—Gamma-Ray, Spectrum analysis, Non-linear least-square fitting.

## I. INTRODUCTION

FOR the past three decades, conventional computational techniques have been in use for the identification and quantification of radioisotopes through the analysis gamma-ray spectrum.

In every quantitative application of gamma-ray spectrometry, one of the most important issues to be addressed is the identification in the spectra of the peaks associated with gamma-ray transitions and then performing the fitting process for precise determination of the position and peak area in the spectrum [1-3].

In the review of literature different programs have been designed depending on the types of the mathematical method in the fitting technique. Mariscot *et al.* [4] have suggested a fitting subroutine which follows the linearization to estimate the required derivatives, and the Newton-Raphson method to occur the iterations in the fitting; while Helmer *et al.* [5] have used Gauss equation and truncated Taylor series.

According to Rotti *et al.* [6], the line-shape calculation and the fitting procedure was performed by running the computer codes SAMPO (and its modification versions SAMPO76, SAMPO80, SAMPO90)[7], that is one of the widely used computer programs in this field that features algorithms for automatic peak fitting which follows an iterative gradient minimization searching with variable metric. Then in the latest years some software were also widely used to analyze the gamma spectra, like Genie 2000, SAANI and VISPECT, Cambio [7].

In the present study, a FORTRAN code was programmed to use a non-linear least square fitting with Levenberg-Marquardt

(LM) method to perform analysis of the gamma-ray spectrum of Hp(Ge) detector.

## II. DATA ANALYSIS

In the present study the data was accumulated in a mountainous region of Iraqi Kurdistan (Erbil). The data were recorded with a high-pure germanium detector HP(Ge), of active volume (62 cm<sup>3</sup>) with an efficiency of about (15%) and resolution of (2.1 KeV) for the (1332.5 KeV) gamma-ray line of Co<sup>60</sup>, preamplifier model (120-4), spectroscopy amplifier model 2020 (Canberra), multichannel analyzer with (4096) channel {series-85 (Canberra origin)} and the IBM proprinter model 5514-2.

The first step in the process of gamma-ray spectrum analysis is indication of the individual peaks in the spectrum. Then Gaussian function has been used as a mathematical model that is a non-linear function, to perform process of peak fitting for finding the best parameters of the Gaussian. Then the second step begins to analyze the gamma-ray spectrum by determining the energy and relative intensities of the individual strong peaks [9].

## III. MATHEMATICS OF THE LEVENBERG-MARQUARDT FITTING

The fitting process of n-data on the gamma-ray peak (i.e.,  $y_i, i = 1, 2, 3, \dots, n$ ) requires to use a mathematical model  $y(x_i, p)$ . Thus, from the definition of Chi-square we have [9-10]:

$$\chi^2(p) = \sum_{i=1}^n \omega_i [\varepsilon_i(p)]^2 \quad (1)$$
$$\varepsilon_i(p) = y_i - y(x_i, p)$$

Here (p) is used for the parameters of function  $y(x_i, p)$  and

$\omega_i$  represents the weight such that:

$$\omega_i = \begin{cases} 1/\sqrt{|y_i|}, & y_i \neq 1 \\ 1, & y_i = 1 \end{cases} \quad (2)$$

As shown in Fig.(3-1), the function of gamma-ray line  $y(x_i, p)$  can be constructed from three functions: main Gaussian  $G(x_i)$ , a step background  $B(x_i)$ , and tailing Gaussian  $T(x_i)$  in the low energy region. Thus,  $y(x_i, p)$  can be expressed as:

$$y(x_i, p) = G(x_i) + T(x_i) + B(x_i) \quad (3)$$

A. H. Fatah, is with Sulaimani University, College of Science, Physics Department, Kurdistan Region, Sulaimani (e-mail: aziz.fatah@univsul.net).

A. H. Ahmed, is with the Salahadeen University, College of Science, Physics Department, Kurdistan Region, Arbil (e-mail: aha66sara@yahoo.com).

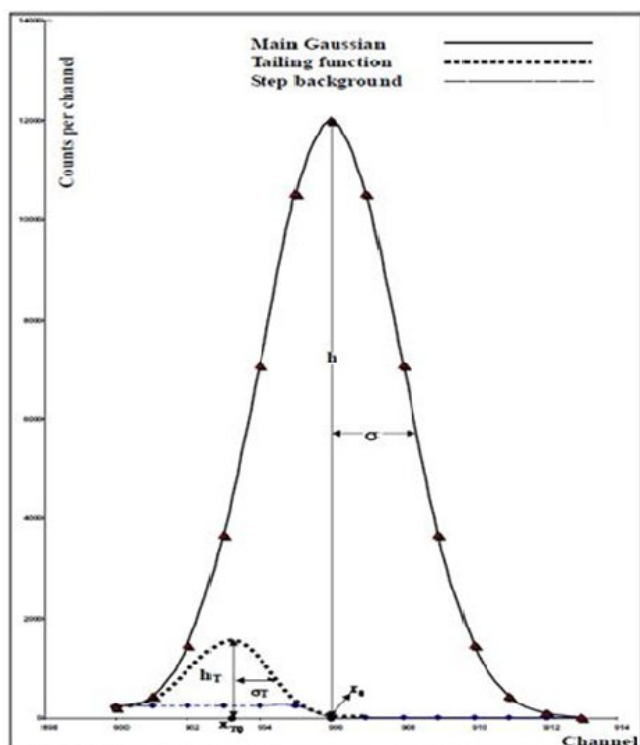


Fig. 1: A typical gamma-ray peak with its components, step and tailing functions

The components, main Gaussian, tailing Gaussian, and step functions are given by [6]:

$$\left. \begin{aligned} G(x_i) &= h e^{-(x_i - x_0)^2 / 2\sigma^2} \\ T(x_i) &= h_T e^{-(x_i - x_{T0})^2 / 2\sigma_T^2} \\ B(x_i) &= \begin{cases} y(x_1), & x < x_0 \\ y(x_n), & x \geq x_0 \end{cases} \end{aligned} \right\} \quad (4)$$

By noting that the parameters  $h, x_0$ , and  $\sigma$  symbolize to the respective height, centroid, and standard deviation of the main Gaussian; while  $h_T, x_{T0}$ , and  $\sigma_T$  are used to the tailing Gaussian.

From the fact that the function  $y(x_i, p)$  is non-linear in parameters, it is convenient to use Taylor expansion to linearize both  $\chi^2(p)$  and  $y_i(x_i, p)$  in eqs.(1 and 3) to be:

$$\chi^2(p) = \chi_o^2(p) + \sum_{j=1}^m \nabla_j [\chi_o^2(p)] \delta p_j \quad (5)$$

$$\begin{aligned} y(x_i, p) &= y_o(x_i, p) + \sum_{j=1}^m \nabla_j [y_o(x_i, p)] \delta p_j \\ &+ \frac{1}{2} \sum_{j=1}^m \sum_{k=1}^m \nabla_{kj}^2 [y_o(x_i, p)] \end{aligned} \quad (6)$$

Knowing that  $\chi_o^2(p)$  is determined from eq.(1) with replacing  $y(x_i, p)$  by  $y_o(x_i, p)$ , and  $\delta p_j$  is the step length.

To get the best values of the parameters,  $\chi^2(p)$  must be minimized to evaluate the local minimum point from relation [11]:

$$\nabla_k \chi^2(p) = \nabla_k \chi_o^2(p) + \sum_{j=1}^m \nabla_{kj}^2 \chi_o^2(p) \delta p_j = 0 \quad (7)$$

Eq.(7) is a differential equation that can be solved to find the step length  $\delta p_j$  [9], or

$$\delta p_k = - \frac{\nabla_k \chi_o^2(p)}{\sum_{j=1}^m H_{kj} \chi_o^2(p)} \quad (8)$$

In such a way that  $\nabla_k \chi_o^2(p)$  and  $H_{kj} \chi_o^2(p)$  are the components of the respective gradient and the Heissian matrices [11-12],

$$\left. \begin{aligned} \nabla_k \chi_o^2 &= 2 \sum_{i=1}^n J_{ij} F_i \\ H_{kj} \chi_o^2(p) &= 2 \sum_{i=1}^n (J_{ij} J_{ik} + F_i H_{kj}) \end{aligned} \right\} \quad (9)$$

With its corresponding matrix form:

$$\left. \begin{aligned} \nabla \chi_o^2(p) &= 2 J^T(p) \times F(p) \\ H \chi_o^2(p) &= 2 [J^T(p) \times J(p) + F^T(p) \times H(p)] \end{aligned} \right\} \quad (10)$$

Here, F and the Jaccobian matrix J, are  $(1 \times n)$  and  $(n \times m)$  matrices respectively, such that:

$$\left. \begin{aligned} F_i &= \sqrt{\omega_i} \varepsilon_i^o(p) \\ J_{ij} &= \frac{\partial F_i}{\partial p_j} = \sqrt{\omega_i} \frac{\partial \varepsilon_i^o(p)}{\partial p_j} \end{aligned} \right\} \quad (11)$$

By substituting eq.(10) in eq.(8), the step length of the fitting becomes:

$$\delta p = - [J^T \times J + F^T \times H]^{-1} J^T \times F \quad (12)$$

That is equivalent to the formula:

$$\delta p^k = -\alpha^{-1} (p^k) \times \beta (p^k) \quad (13)$$

Both matrices  $\beta, \alpha$  are two  $(1 \times m)$  and  $(n \times m)$  matrices respectively, which have the elements:

$$\left. \begin{aligned} \beta(p) &= \frac{1}{2} \nabla_o^2(p) \\ \alpha(p) &= \frac{1}{2} H \chi_o^2(p) \end{aligned} \right\} \quad (14)$$

In the search direction, for  $k^{\text{th}}$  iteration with step length  $\delta p^k$ , the Newton method is used to reach the local minimum  $\delta p^{k+1}$ , or

$$\delta p^{k+1} = \delta p^k + \Delta p^k \delta p^k \quad (15)$$

Here,  $\lambda^k I$  is the step size which takes the small positive values.

The (LM) method is a type of modified Newton-Gauss algorithm of eq.(15). The method involves an additive square diagonal matrix ( $\lambda^k I$ ) for the Hessian matrix ( $\alpha$ ) in eq.( 15) to replace the negative or small eigenvalues of  $\alpha$  by reasonable positive ones. The resulting step length is given by [12]:

$$\delta p^k = -[\alpha(p^k) + \lambda^k I]^{-1} \times \beta(p^k) \quad (16)$$

(I) is a unit matrix with the same order of  $\alpha$ , and  $\lambda^{k+1} > \lambda^k$  takes the values such that  $\lambda^k > 0$ .

The basis of (LM) method is to control the step length ( $\delta p$ ), so that it decreases monotonically in length as ( $\lambda^k$ ) increases.

However, if the value of ( $\lambda^k$ ) is changed, one has to calculate the new ( $\delta p^k$ ) and the iteration procedure for ( $\Delta p^k$ ) requires selecting ( $\lambda^k$ ), such that [13],  $\lambda^{k+1} > \lambda^k$

To estimate ( $\delta p^k$ ), the elements of  $\beta$  and  $\alpha$  must be determined from eqs.(10-14):

$$\left. \begin{aligned} \beta_j &= -\sum_{i=1}^n \omega_i \varepsilon_i^o [y_o(x_i, p)] \\ \alpha_{jk} &= \sum_{i=1}^n \omega_i \varepsilon_i^o \nabla_j [y_o(x_i, p)] \nabla_k [y_o(x_i, p)] \end{aligned} \right\} \quad (17)$$

According to eq.(17) the diagonal elements of ( $\alpha$ ) are given by:

$$\alpha_{jj} = \alpha_{jj}(1 + \lambda) \quad (18)$$

Computationally, at least two problems are involved in the (LM) method: the first is the need for solving a linearized system at each step, and the second is evaluating the derivatives at each step. One can eliminate most of the derivatives by using the differences (non-analytical method)[9]:

$$\frac{\partial y_o(x_i, p)}{\partial p_j} = \lim_{\Delta p \rightarrow 0} \left[ \frac{y_o(x_i, p_j + \Delta p_j) - y_o(x_i, p_j)}{\Delta p_j} \right] \quad (19)$$

So that the step size is so small that causes to maintain rapid convergence.

#### IV. PEAK CALCULATION

After performing the process of fitting, the peak parameters ( $h$ ,  $x_o$  and  $\sigma$ ) can be found; then from the peak centroid ( $x_o$ ) and from the energy calibration the photopeak energy can be evaluated from [8,14]:

$$E = W_1 + W_2 x_o + W_3 x_o^2 \quad (20)$$

with the uncertainty,  $\sigma(E)$

$$Er(E) = W_2 x_o + W_3 x_o^2 \quad (21)$$

And similarly, calibration of the standard deviation that:

$$\left. \begin{aligned} \sigma &= G_1 + G_2 x_o + G_3 x_o^2 \\ \sigma &= FWHM/2.355 \end{aligned} \right\} \quad (22)$$

Where **FWHM** is the Full Width at Half Maximum;  $W_1$ ,  $W_2$  and  $W_3$  are constants of energy calibration; while  $G_1$ ,  $G_2$  and  $G_3$  are constants of calibration of standard deviation.

In similar way the efficiency of the peak ( $\varepsilon_f$ ) and peak energy (**E**) are combined according to efficiency calibration relation:

$$\varepsilon_f = z_1 E^{-z_2} \quad (23)$$

Where  $z_1$  and  $z_2$  are constants of efficiency calibration for the detector.

By subtracting background before peak fitting, there occurs simplification of the shapes of experimental peaks that reduces the required fitting time. Therefore, after the background estimation (which is not fitted or its values before and after fitting are equal) had been made and the background subtraction performed under the event channels, analytic fits were then made to result the interest parameters [15-16].

From the fitting process the best values of the parameters can be found, and then putting them in eq.(3), area of the peak (A) can be evaluated from[9-10]:

$$A = \int_{-\infty}^{\infty} y(x) dx \quad (24)$$

Where (h) and ( $\sigma$ ) are the height and standard deviation of the Gaussian respectively. And the percentage error in area  $Er(A)$  is calculated from [17]:

$$Er(A) = 165 \frac{\sigma(A)}{A} \quad (25)$$

Knowing that  $Er(A)$  is the estimation of uncertainty in the peak area that is calculated from [19]:

$$\sigma(A) = \sqrt{A+B} \quad (26)$$

Since(B) represents area of the counts under the background.

The intensities of individual gamma-lines ( $I_n$ ) in a spectrum are characterized by the corresponding peak area (A) and efficiency ( $\varepsilon_f$ ) [8-10], or

$$I_n = \frac{A}{\varepsilon_f} \quad (27)$$

And thus, the percentage error in the intensity  $Er(I_n)$  is calculated from:

$$Er(I_n) = \frac{Er(A)}{\varepsilon_f} \quad (28)$$

But in addition to the energies of the gamma lines, the interested quantities in gamma-ray spectrum analysis is the relative intensity of the peaks, which can be obtained in such a way that a line for each element in the spectrum must be specified to be taken as a line with intensity assumed to be

100%, then the intensity of all other gamma-lines belonging to the same element are measured relative to that line. Therefore, the relative intensity ( $I_\gamma$ ) for any line with intensity ( $I_n$ ) and belonging to a standard line with intensity ( $I_{st}$ ) is written as [10]:

$$I_\gamma = \frac{I_n}{I_{st}} \quad (29)$$

programs with the boundary channels of the peaks separately, the parameters of the peak shape functions and backgrounds were determined.

For the utilized spectrum which contains 4095 channels, see Fig.1, a computer program with Fortran language has been developed for calculating the physically meaningful Gaussian functions. Then after running the program, the requirements of spectral analysis on the present data was made with general purposes of nonlinear least-square fitting (Levenberg-Marquardt) method by making the individual peak analysis for

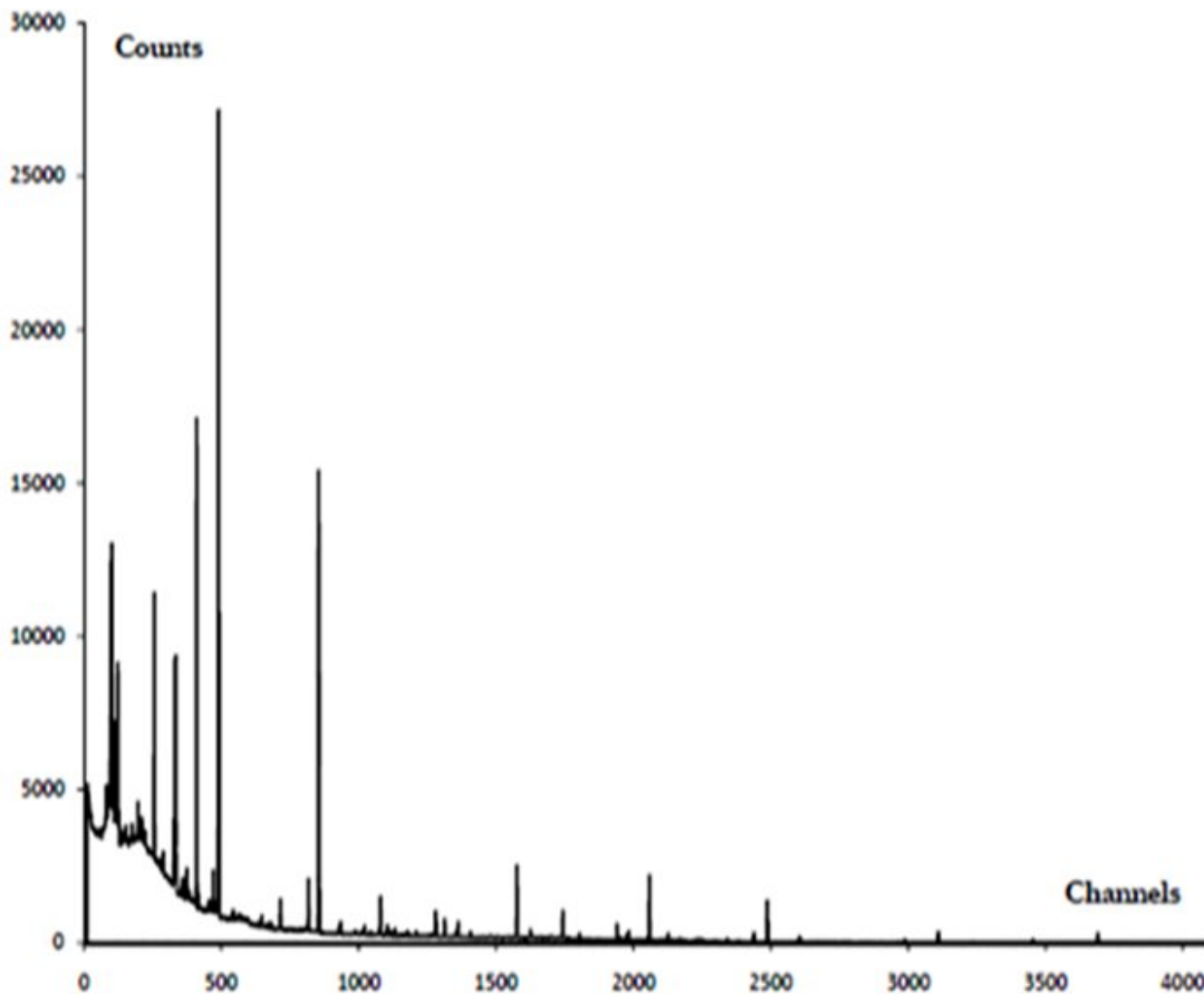


Fig. 2: The whole spectrum of Hp(Ge) detector for the channel ranges (1-4095)

$$Er(I_\gamma) = \frac{Er(I_n)}{\epsilon f} \quad (30)$$

#### V. RESULTS AND DISCUSSION

The peak shape model presented is a powerful tool for a precise analysis of the gamma-ray peaks in the pulse height spectrum of Hp(Ge) spectrometer. By applying the fitting

The purpose in the spectrum analysis is usually to determine energies and intensities of nuclear radiation which are related to free parameters (peak counts, positions and widths) in the Gaussian function. After performing fitting process, the peak parameters have been found, and then for each line of gamma ray the centroid was putted in eqs.(20-21) to evaluate the peak energy with its percentage error. Thus, from the efficiency calibration, in eq.(23), the efficiency was obtained and after

then from the full description of the photopeak, the integration (continuous) method was proposed, in eq.(24), to determine area under the peak. As the final process of calculation, both area and efficiency were substituted in eqs.(27-28) to get the line intensity and its error estimation. Hence, for the strong lines the relative intensities with their corresponding errors have been obtained from eqs.(29-30) A typical gamma-ray full energy peak having a very low background was carefully studied to indicate an analytical expression, which would very closely represent its shape. Accordingly, the ratio between the peak height and its background (i.e., peak-to-background ratio, PB) has been proposed to describe the strong peaks (having  $PB > 2$ ) in the spectrum. Therefore, one of the typical aspects of differences in the results is what might be described as a small peak-to-background ratio (PB)[4,10]. This is a case where the peak in the data is riding on a very high background, and the ratio of the highest point of the peak to the average of the baseline level is a very nearly one.

Table 1 shows the calculated values of some of the interesting parameters, peak areas, percentage errors in the areas, peak-to-background ratios (PB), and the peak boundaries before the fitting for the choosing strong lines (23 peaks) in the spectrum. So one obtains that the peak area evaluation depends mostly on the base line height and the percentage error in area goes up as (PB) decreases because the statistics are poorer; thereby, the table also shows that the strong peaks usually have large values of peak-to-background ratios ( $PB > 2$ ) and small errors in areas. After the fitting process, the parameters of the main Gaussian have been obtained and they are listed in Table 2.

TABLE I SOME OF THE INTERESTING PHYSICAL QUANTITIES OF THE STRONG LINES IN THE SPECTRUM

No	A	$\Delta A\%$	PB	Peak boundary	
				Initial	Final
01	14309.1	01.35	03.38	0327	0332
02	33539.6	01.96	13.22	0407	0413
03	55843.6	00.70	29.43	0484	0493
04	03782.5	02.32	03.54	0814	0820
05	37711.3	00.01	32.93	0851	0858
06	03203.3	04.59	05.30	1074	1082
07	02402.7	00.06	04.53	1274	1285
08	01706.9	01.48	03.91	1309	1319
09	01382.0	00.97	02.64	1359	1366
10	07140.9	00.06	14.31	1572	1582
11	02562.7	01.12	05.10	1738	1747
12	01578.5	06.06	05.34	1936	1944
13	00546.8	04.89	02.91	1970	1977
14	00945.7	02.33	03.46	1976	1986
15	00373.1	03.15	02.78	2338	2346
16	00984.8	01.95	08.19	2434	2444
17	04998.4	00.03	40.25	2482	2492
18	00114.7	04.26	02.29	2588	2596
19	00648.8	02.88	05.90	2599	2608
20	00331.4	01.75	06.26	2983	2994
21	01290.1	00.60	25.62	3104	3115
22	00328.1	01.20	3.769	3451	3458
23	01156.9	02.30	25.47	3686	3696

TABLE II THE PARAMETERS OF THE STRONG LINES IN THE SPECTRUM

No	Peak parameters		
	Height	Centroid	Width
01	07772.0±99.46	0329.36±0.009	0.73±0.0080
02	16034.7±95.87	0409.58±0.005	0.81±0.0040
03	25993.2±97.47	0489.93±0.004	0.85±0.0030
04	01649.7±40.87	0817.12±0.022	0.90±0.0190
05	14800.8±68.46	0853.93±0.006	1.01±0.0040
06	01173.3±30.95	1078.60±0.026	1.08±0.0240
07	00764.3±27.74	1280.31±0.036	1.03±0.0320
08	00529.6±81.74	1312.72±0.047	1.18±0.0420
09	00506.8±22.98	1362.24±0.044	0.97±0.0400
10	02368.9±38.40	1576.08±0.016	1.16±0.0140
11	00877.5±25.82	1742.87±0.031	1.11±0.0270
12	00526.0±19.35	1940.11±0.030	1.16±0.3520
13	00156.6±12.03	1973.85±0.098	1.27±0.0900
14	00299.4±16.29	1982.81±0.058	1.06±0.0520
15	00100.2±10.93	2342.03±0.103	0.85±0.0920
16	00278.3±12.59	2438.11±0.056	1.37±0.0480
17	01247.8±27.16	2487.72±0.026	1.27±0.0200
18	00127.8±10.99	2591.66±0.298	1.58±0.2740
19	00174.8±11.24	2604.12±0.076	1.15±0.0660
20	00084.5±06.56	2988.38±0.112	1.56±0.0950
21	00345.8±12.64	3109.55±0.046	1.47±0.0380
22	00039.6±06.66	3455.17±0.239	1.24±0.1970
23	00292.9±11.27	3690.29±0.052	1.57±0.0420

This large appearance of percentage errors in the weak peak areas is due to that these peaks cannot be represented accurately by Gaussian functions only, but it must do additional corrections in the Gaussians or other complex representations to define those photopeaks.

In other words, it states that the used function gives a better fit to the experimental full energy strong peaks. Consequently the detection of very small peaks in the spectrum is complicated by the appearance of fraudulent peaks which are in nearly noise and fitting of these peaks are very sensitive to the height of the background under the peaks. For this reason, the peaks whose percentage errors in areas exceed (23%) they would very likely not considered as real peaks in the spectrum and would be removed from the fit.

The final columns of the table show the peak boundaries, i.e. initial peak and final channels; and the peak parameters, i.e. height, centroid, and with their corresponding errors.

The peak energies and relative intensities (intensities normalized to (100) for the standard lines) which are common feature in many environmental radiation measurement programs have been calculated after fitting the data peaks separately. The accuracy of such results is especially bad if the peak of interest is small and on the tail of a large one. The percentage area contribution on the tail function (T) is dependent on the fitting used in the analysis.

The computed results, relative intensities, are shown in Table 3 and compared with those published in the Nuclear Data Sheets (N.D.S) [18-22]. The comparison in Table 3 illustrates the existence of good accuracy in the obtained results because they are in small errors. Moreover, the present

$\gamma$ -ray intensities agree well with those of (N.D.S) [18-22], that considered as standard values. The agreement is more obvious for the strong lines, i.e., in ideal situations, the peak area is mostly well resolved and has large peak-to-background ratios.

It is important to be known the two lines with the energies of (662 KeV) and (1461 KeV) from  $^{137}\text{Cs}$  and  $^{40}\text{K}$  nuclides, respectively, were clearly observed that is impossible to identify their relative intensities because they are members of the ((Non-Serious Radioactive Nuclide In Nature)). Other types of these nuclides are not found either because of their low energy or their extremely low natural abundance.

TABLE III COMPARISON OF THE COMPUTED  $\gamma$ -RAY RELATIVE INTENSITIES FOR THE STRONG LINES WITH WHOSE REPORTED BY THE NUCLEAR DATA SHEETS (N.D.S)

No.	Nuclides	PB	Present work		N.D.S [18-22]
			$E_\gamma$ (KEV)	$I_\gamma$	
01	B <sup>†</sup>	03.38	0238.54±0.006	100.00±0.316	100.00
02	A	13.22	0295.29±0.004	051.45±0.016	051.74
03	E	29.43	0352.12±0.003	100.00±0.014	100.00
04	B	03.54	0583.55±0.015	085.15±0.099	085.20
05	A	32.93	0609.73±0.004	100.00±0.024	100.00
06	B	05.30	0768.48±0.015	010.55±0.015	010.59
07	A	04.53	0911.13±0.025	100.00±0.255	100.00
08	A	03.91	0934.05±0.033	006.63±0.029	006.86
09	B	02.64	0969.07±0.031	060.68±0.350	060.80
10	A	14.31	1120.28±0.011	032.68±0.010	032.62
11	B	05.10	1238.22±0.021	012.82±0.024	012.83
12	E	05.34	1377.68±0.028	008.66±0.033	008.72
13	C	02.91	1401.53±0.069	003.06±0.072	003.00
14	C	03.46	1407.87±0.040	005.31±0.052	005.37
15	B	02.78	1661.83±0.073	002.51±0.120	002.49
16	C	08.19	1729.76±0.039	006.75±0.046	006.60
17	F	40.25	1764.82±0.018	034.38±0.017	034.54
18	C	02.29	1838.30±0.011	000.81±0.234	000.83
19	E	05.90	1847.11±0.053	004.68±0.061	004.60
20	B	06.26	2118.72±0.079	002.56±0.103	002.62
21	B	25.62	2204.36±0.032	010.93±0.040	010.83
22	C	3.769	2448.41±0.166	003.02±0.103	003.36
23	D	25.47	2614.78±0.036	100.00±0.460	100.00

• A:  $^{231}\text{Th}$ , B:  $^{228}\text{Th}$ , C:  $^{214}\text{Bi}$ , D:  $^{214}\text{Po}$ ,  
E:  $^{212}\text{Bi}$ , F:  $^{208}\text{Pb}$ , G:  $^{212}\text{Po}$

In addition, two other obvious peaks are seen in the spectrum that represent disperse  $\gamma$ -ray lines, are (741.304 KeV) belonging to  $^{214}\text{Po}$  and (1001.26 keV) belonging to  $^{207}\text{Tl}$  and  $^{234}\text{U}$ , were identified and ascribed qualitatively. The disperse  $\gamma$ -ray lines included:

- 1- Low intensity  $\gamma$ -ray lines.
- 2- Overlapping lines in the low-energy region.
- 3- Lines with unknown origins.
- 4- Fluorescence lines (have X-ray contributions).

The spectrum contains also some other obvious peaks whose energies were determined and belonged to X-ray, so they are of no interest in the present work.

Furthermore, the inclusion of this analysis would, in practice, to break down in some peaks as a result of controlling

their values (the peak) only by a few channels (narrow region,  $n < 5$ , n is the number of the counts on the peak) that leads to appear (floating point error, overestimated) in the running procedure. It express that, the computer analysis is less sensitive to resolution than analysis by hand for this photopeaks in the running procedure.

## REFERENCES

- [1] G. S. Zahn, Frederico A. Genezini, MauricioMorales,, 2009 International Nuclear Atlantic Conference - INAC 2009 Rio de Janeiro,RJ, Brazil, September27 to October 2, 2009.
- [2] R. E. Abdel-Aal, IEEE TRANSACTIONS ON NUCLEAR SCIENCE, VOL. 45, NO. 1, (1998)1.
- [3] P.H.G.M. Hendriks, J. Limburg, R.J. de Meijer, Journal of Environmental Radioactivity, 53 (2001) 365.
- [4] M.A. Mariscotti ,Nucl.Inst.and Methods, 50(1967) 309-320.
- [5] R.G. Helmer, R.I. Heath, M. Putnam and D.H. Gipson, Nucl.Inst.and Methods, 57(1967) 46-57.
- [6] J.T. Routti and S.G. Prussin, Nucl.Inst.and Methods, 72(1969) 125-142.
- [7] M. Blaauw, Nucl.Inst.and Methods, A333 (1993) 548-552.
- [8] A. H. Fattah, JZS, 11(1), Part A( 2008 )9.
- [9] Philip R. Bevington, Data Reduction and Error Analysis for the Physical Sciences, (McGraw-Hill,2003).
- [10] P. C. Gregory, Bayesian Logical Data Analysis for the Physical Sciences, Cambridge University Press (2005).
- [11] E. Philip Gill and Walter Murray , Siam J. Numer. Anal., 15,2,(1979)
- [12] M. A. Bhatti, Practical Optimization Methods, Springer-Verlag New York (2000).
- [13] W. Murray, Numerical Methods for Unconstrained Optimization,(New York,1972).
- [14] T.A.E.C.Pratt.,Luther.M.L.,Nucl.Inst.andMethods,92(1971)141-157.
- [15] Wang Liyu, Appl.Radiat.Isot.,Vol.40,No.7,(1989)575-579.
- [16] Ciftcioglu özer, Nucl.Inst.and Methods, 174(1980) 209-220.
- [17] Camberra, Technical Reference Manual 1088, (1988).
- [18] K.S. Toth, Nucl.Inst.and Methods, Vol.21, No.4, August (1977).
- [19] M.J. Martin, Nucl.Inst.and Methods, Vol.27, No.4, August (1979).
- [20] M.R. Schmorak, Nucl.Inst.and Methods, Vol.40, No.1, September(1983).
- [21] M.J. Martin, Nucl.Inst.and Methods, Vol.47, No.4, April (1986).
- [22] M.J. Martin, Nucl.Inst.and Methods, Vol.49, No.1, September (1986).